

## Observation of Site-Specific Electron Emission in the Decay of Superexcited O<sub>2</sub>

A. V. Golovin,<sup>4,2</sup> F. Heiser,<sup>2</sup> C. J. K. Quayle,<sup>1</sup> P. Morin,<sup>3</sup> M. Simon,<sup>3</sup> O. Gessner,<sup>2</sup> P.-M. Guyon,<sup>1</sup> and U. Becker<sup>2</sup>

<sup>1</sup>Laboratoire des Collisions Atomiques et Moléculaire Bat 351, Université Paris Sud, 91405 Orsay, France

<sup>2</sup>Fritz-Haber-Institut der Max-Planck-Gesellschaft, D-14195 Berlin, Germany

<sup>3</sup>Laboratoire pour l'Utilisation du Rayonnement Electromagnetique Bat 209d, Université Paris Sud, 91405 Orsay, France

<sup>4</sup>Institute of Physics, St. Petersburg State University, Petrodvorets, 198904 St. Petersburg, Russia

(Received 21 July 1997)

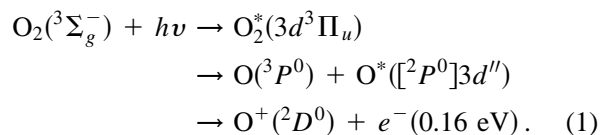
The photodissociation of superexcited O<sub>2</sub><sup>\*</sup> to O(<sup>3</sup>P) and O<sup>\*</sup>([<sup>2</sup>P<sup>0</sup>]3d'') atoms, with subsequent autoionization to O<sup>+</sup>(<sup>2</sup>D<sup>0</sup>) + e<sup>-</sup> (0.16 eV) at 22.36 eV photon energy, was studied by a new method: angle resolved photoelectron-photoion coincidence spectroscopy. A position-sensitive detector was used to measure the three components of the fragment ion velocity. When the excited atom autoionizes it emits an electron preferentially along the photodissociation axis, with a 12% greater probability to be emitted away from the receding ground-state atom than towards the latter, pointing to possible intramolecular scattering of the electron on its way out. [S0031-9007(97)04740-6]

PACS numbers: 33.80.Gj, 33.60.Cv

The valence photoionization yield spectrum of O<sub>2</sub> shows many sharp and broad structures (resonances), some of which have been assigned to Rydberg series converging to excited states of the molecular ion [1]. Excitation of such resonances or superexcited states may result in the fragmentation of the molecule in neutral nuclear fragments O + O<sup>\*</sup> (dissociation-predissociation) or in the creation of an ion-electron pair O<sub>2</sub><sup>+</sup> + e<sup>-</sup> (ionization-autoionization) [2,3]. In most of the experiments, only the energy state of the products were measured but not their momentum [2-4]. In a photoionization process, the photon actually transfers its angular momentum to the molecule and much more information on this basically anisotropic process is obtained if one measures the vector correlations between the electron, the fragment ion, and the electric vector of the light. The electron angular distribution in the laboratory frame is an incoherent superposition of electron distributions of all randomly oriented molecular axis directions. The new technique of angular-resolved photoelectron-photoion coincidence spectroscopy makes it possible to measure the amplitudes and phases of the photoelectron continuum wave function in the molecular frame. The method was first introduced by Golovin and co-workers [5,6] for valence photoionization, followed by Shigemasa *et al.* [7] who studied inner-shell photoionization. Recently, Guyon *et al.* [8] investigated the photoelectron-photoion coincidence spectrum of O<sub>2</sub>, and observed a strong correlation between the velocity vectors of the electron and the fragment O<sup>+</sup> ion when the molecule was excited at 22.36 eV. From the analysis of the O<sup>+</sup> time-of-flight (TOF) peak shape, which is determined by the distribution of the O<sup>+</sup> velocity component along the spectrometer axis, they concluded that the Auger electron emitted by an excited fragment atom was preferentially directed along the photodissociation axis suggesting that it might be emitted as a σ wave. But the above experiment did not provide any information upon the distribution of the

velocity projections in the plane perpendicular to the spectrometer axis.

The aim of the present investigation was to measure the 3D distribution of the O<sup>+</sup> fragments in coincidence with electrons emitted in a fixed direction upon excitation of O<sub>2</sub> at 22.36 eV. The process under investigation is illustrated on the potential energy curve diagram in Fig. 1. Three steps are considered:



The photon excitation energy 22.36 eV was chosen to lie above the dissociation limit of O(<sup>3</sup>P<sup>0</sup>) + O<sup>\*</sup>([<sup>2</sup>P<sup>0</sup>]3d'') at 22.22 eV [9]. On their way towards dissociation, the nuclei reach the point where the Rydberg neutral potential energy curves cross the asymptotic limit of the B<sup>2</sup>Σ<sub>g</sub><sup>-</sup> ionic state curve. From this point autoionization via recoupling of the core [10] becomes possible for 3d excited O<sup>\*</sup> producing O<sup>+</sup>(<sup>2</sup>D<sup>0</sup>) fragment ions. The 4s excited state lies just below threshold for autoionization and will not contribute to the signal in an electron analyzer, rather it will decay via fluorescence [2,3].

This Letter reports the first experimental, three-dimensional study of a photofragment ion velocity vector distribution correlated with valence Auger electrons emitted in a fixed direction. The principle of the measurement is the following: Because of the intrinsic anisotropy of the molecular photoabsorption process the ensemble of excited molecules is highly aligned. As a result of this alignment, being described by the molecular anisotropy parameter β<sub>m</sub>, the fast dissociation of the excited molecule is also anisotropic. The dissociation time may approximately be determined from the widths of the autoionizing resonances of 0.04 eV which is 2 orders of magnitude larger than the typical rotational widths of

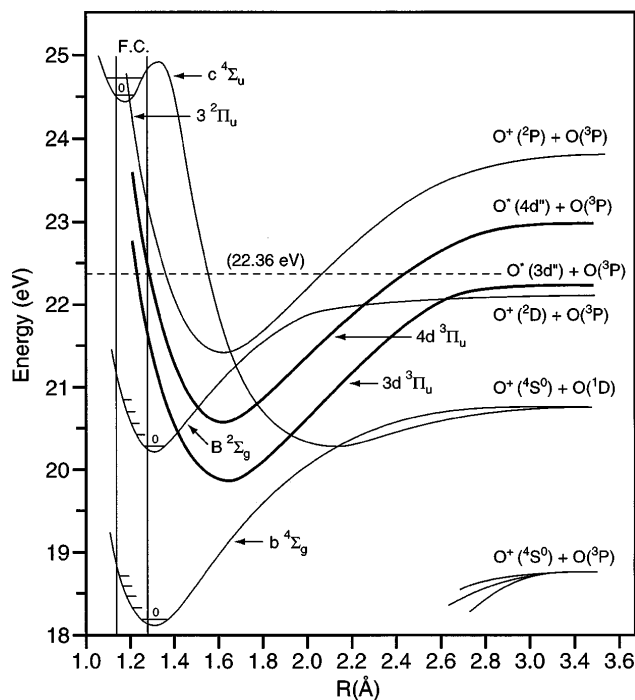


FIG. 1. Potential energy curves for  $O_2$  and  $O_2^+$  with dissociation continua depicted for excited and ionized oxygen atoms along with the Franck-Condon (F.C.) regime.

several  $\mu\text{eV}$ . Under this condition, the dissociation of the molecule is much faster than its rotation, giving rise to ionic fragment emission along the initial molecular axis direction. These circumstances are known as axial recoil condition, making it possible to derive the molecular axis distribution characterized by the absorption anisotropy  $\beta_m$  [11] from the angular distribution of the corresponding fragment ions. Therefore, angle-resolved ion-electron coincidence measurements using a fixed angle electron detector have to take this nonisotropic axis distribution into account because it will directly be folded into the coincident electron molecular axis distribution. Figure 2 gives a schematic representation of the described experiment, e.g., for a near perpendicular transition, in terms of angular patterns representing the fragmentation angular distribution in the laboratory frame and the electron angular distribution in the molecular frame depending on the molecular axis direction only. The doughnutlike structure, corresponding to an axis distribution with  $\beta_m = -0.56 \pm 0.15$ , is taken from a coincidence measurement with zero volt electrons which was in good agreement with former measurements [8]. The unfolded coincident ion angular distribution which in our case is equivalent to the electron angular distribution in the molecular frame  $I_{\text{mol}}^e$  in case of polar symmetry is shown inside the doughnut. The specific form of this angular distribution will be discussed later in the context of the data analysis. First, we will make a brief description of the experimental technique, more details will be given in a future publication.

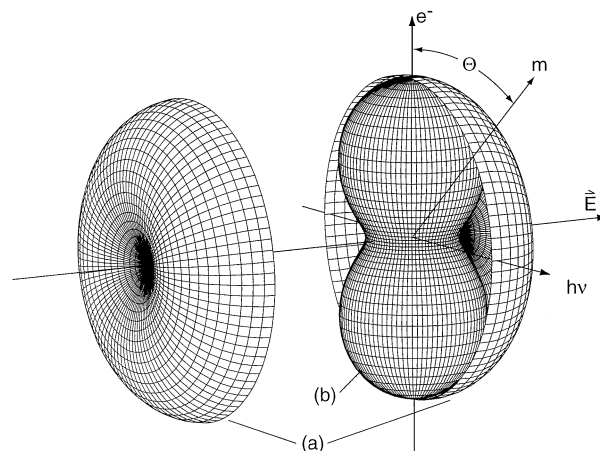


FIG. 2. (a) The fragmentation angular distribution  $m$  in the laboratory frame, determined by the photon beam direction  $h\nu$  and the electric vector  $\vec{E}$ , along with (b) the electron angular distribution in the molecular frame for an axis selected parallel to the electron spectrometer axis  $e^-$ . The latter is in our experimental setup equivalent to an axis distribution  $m$  with respect to a fixed electron detection direction  $e^-$ .

The double time-of-flight spectrometer, previously used to record the electron and ion times of flight in a PEPICO (photoelectron-photoion coincidence) experiment [8,12], was modified with the adjunction of a position-sensitive detector [13] on the ion side as shown in Fig. 3(a). The latter consists of two 40 mm i.d. active area multichannel plates (MCPs) in chevron configuration. The square-shaped anode was equipped with two perpendicular sets, each consisting of 30 conducting lines covering most of the anode area. Each line is connected to an amplifier and discriminator. The impact of an ion on the detector results in the activation of a pair of  $X$ ,  $Y$  lines whose numbers represent the  $X$  and  $Y$  coordinates. The signal from the back of the second MCP served to start a fast decoder system that reads the position. At the same time, the signal goes through a fast multiplexer enabling the detection of two ions in coincidence with an electron. The acquisition cycle is triggered by an electron signal, a synchrotron radiation pulse stops to register the electron time of flight, and four microseconds later ion stop pulses register the ion TOF. The ionization region is defined by the cross section (0.2–0.3 mm) of the light beam and the diameter of the electron extraction aperture (2 mm). The acceptance angle for the electrons was less than  $15^\circ$  being basically determined by apertures in the electron spectrometer. A weak and permanent (0.6 V/cm) electric field is applied for electron extraction. The detection of an electron triggers a pulse generator producing a 15 V/cm ion extraction pulse for about  $2 \mu\text{s}$ . Its amplitude is calculated to fulfill the Wiley MacLaren condition [14]. The resolution of the detection system was 0.1 and 2.5 ns per channel for electron and ion TOF, respectively, and 1.5 mm for position measurement. In the present investigation, electrons of energy less than 0.4 eV emitted

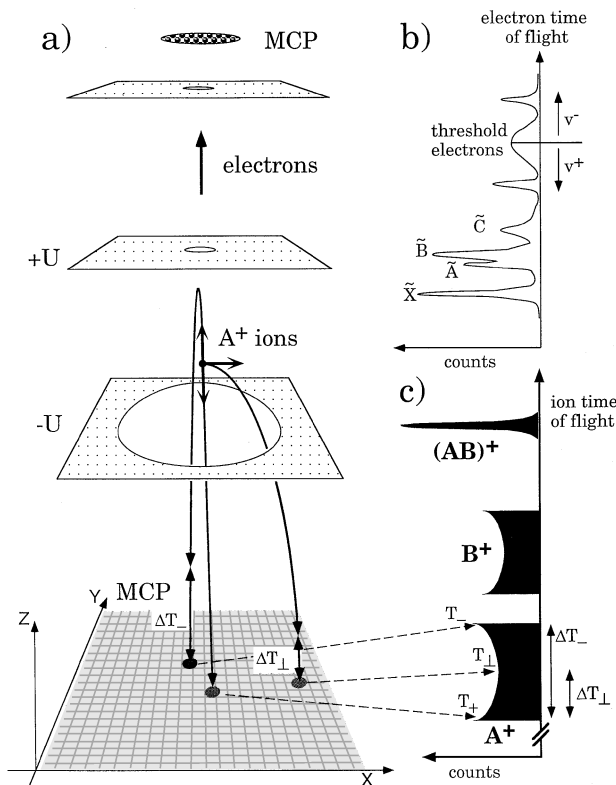


FIG. 3. Principle of the experiment: (a) Scheme of the double TOF analyzer; (b) electron TOF spectrum for O<sub>2</sub> photoionization at photon energy 22.36 eV; (c) ion TOF spectrum.

towards the electron detector [forward (fwd) electrons] or away [backward (bwd) electrons] are selected [Fig. 3(b)]. The molecular ions with a well-defined kinetic energy produce a sharp peak in the TOF spectrum and arrive near the anode center; the O<sup>+</sup> fragments with a distribution of kinetic energies spread over the detector area and produce broader TOF peaks [Fig. 3(c)].

Triggered by an electron, each coincidence event consists of the four numbers  $T_e, T_i, X_i, Y_i$  representing the electron and ion time of flights and the ion arrival position. They are stored in the memory of a PC-based data acquisition system. One raw experimental result consists of a large number, i.e.,  $10^4-10^5$  events registered in about 1 h. To analyze the data, one calculates the electron energy and the three components of the ion momentum. In the following, we analyze two types of coincident events: Forward 0.16 eV and backward 0.16 eV electrons associated with 0.07 eV O<sup>+</sup> fragments. We derived several two-dimensional arrays of the probability distributions of the O<sup>+</sup> velocity vectors for certain electron selections and final fragment ion kinetic energies.

The 3D probability in angular distributions calculated from these two-dimensional arrays for the fwd and bwd selections are shown in Fig. 4. Figure 4(a) shows the O<sup>+</sup> velocity probability distribution associated with forward electrons viewed from the spectrometer axis. It looks quite symmetrical around this axis. Figure 4(c) is a view

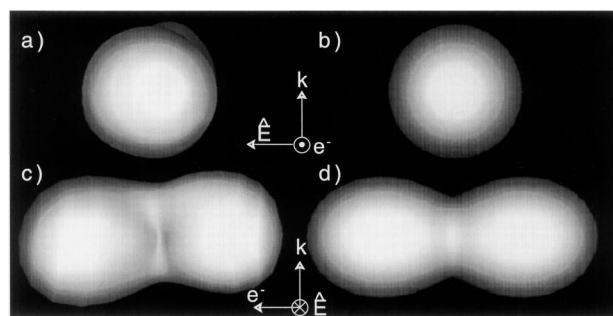


FIG. 4. O<sup>+</sup> coincidences with forward and backward 0.16 eV electrons at photon energy 22.36 eV. 3D views of the probabilities of O<sup>+</sup>: view from the electron spectrometer axis (a), the axis of the electric vector of the light (c), both for forward electrons compared with the result of fitted distributions (b) and (d).

from the molecular beam or polarization axis associated with forward electrons; it shows a distribution elongated along the spectrometer axis. The minimum in the plane of the light propagation and polarization direction is clearly seen. Figures 5(a) and 5(b) correspond to forward and backward electrons, respectively, viewed from the light propagation axis. In both cases O<sup>+</sup> ion emission in the same direction as the electron seems more likely.

Two qualitative observations arise from the inspection of the 3D views. First, O<sup>+</sup> is preferentially emitted along the direction of the electron detection axis. This in turn means that the Auger electron is also emitted preferentially along the dissociation axis of the molecule. This confirms previous observations [8] and suggests that the electron is essentially emitted as a  $\sigma$  wave. Second, the O<sup>+</sup> emission diagram correlated with the electron velocity is asymmetric with respect to the center of photon molecule interaction which is quite surprising considering the symmetry properties of the electric dipole process for homogeneous molecules. One actually observes that the Auger electron is preferentially emitted in the same direction as the O<sup>+</sup> ion and opposite the neutral recessing atom. This phenomenon seems to indicate that the Auger electron may be scattered by the partner oxygen atom on its way out. Our excitation, which is predominantly a perpendicular transition, corresponds to

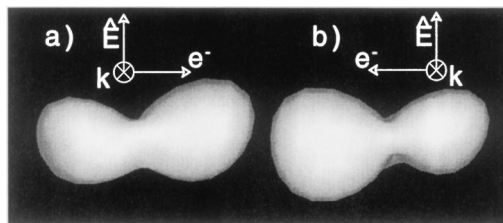
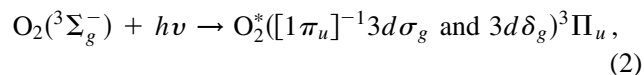


FIG. 5. Views from the light propagation axis for backward (a) and forward (b) electrons.

with subsequent dissociation and autoionization into

$$O(^3P^0) + O^*([1\pi_u]^{-1}\epsilon s\sigma_g, \epsilon d\sigma_g, \text{ and } \epsilon d\delta_g)^3\Pi_u. \quad (3)$$

In order to examine the anisotropy along the electron detection direction quantitatively, we summed the  $O^+$  emission probabilities in two opposite and equal solid angles ( $120^\circ \leq \Theta \leq 180^\circ$ ) and ( $0^\circ \leq \Theta \leq 60^\circ$ ). The ratio of these two numbers was found equal to  $0.86 \pm 0.09$  for forward,  $1.12 \pm 0.1$  for backward, and  $1.01 \pm 0.08$  for threshold electrons giving us confidence in estimating the backward forward anisotropy to be 12%.

As mentioned above, the distributions of the  $O^+$  momentum measured in the laboratory frame carry information on the selection of molecular axes orientations in the absorption process ( $\beta_m$ ) and the subsequent angular distribution of the Auger electron in the molecular frame. If we consider that the dissociation is terminated when the Auger electron is emitted (two-step approximation), its laboratory frame distribution can be written as the product

$$I_{\text{lab}}(\Theta, \Phi) = I_{\text{abs}}(\Theta, \Phi) * I_{\text{mol}}^e(\Theta_e, \Phi_e), \quad (4)$$

where  $I_{\text{abs}}$  is the absorption anisotropy in the laboratory frame and  $I_{\text{mol}}^e$  is the electron distribution in the molecular frame. The absorption anisotropy or angular distribution of the molecular axis measured with respect to an axis perpendicular to the electric vector of the light may be written as

$$I_{\text{abs}}(\Theta, \Phi) = 1 - \frac{\beta}{2} (3 \sin^2 \Theta \cos^2 \Phi - 1), \quad (5)$$

with  $\Theta$  and  $\Phi$  measured with respect to the spectrometer axis direction and, when summed over  $\Phi = 0 - 2\pi$ , it is reducing to formula 4 in [8]. The electron angular distribution is measured in the molecular frame with  $\Theta_e = \pi - \Theta$ ,  $\Phi_e = f(\Theta, \Phi)$ .

Conservation of parity and selection rules tells us that the Auger electron will be emitted as a  $\sigma_g$ ,  $\pi_g$ , or  $\delta_g$  continuum wave. The data strongly support a  $\sigma_g$  wave, the  $\delta_g$  electron would be emitted preferentially perpendicular to the molecular axis, and  $\pi_g$  electrons would be emitted at  $45^\circ$ , two directions in which no ion intensity enhancement is observed. The probability distribution for an electron with gerade symmetry may be expressed in terms of an expansion of even Legendre polynomials.

The fit of the forward distribution with a simple function, containing the first two terms  $1 + \alpha P_2(\cos \Theta)$  only, results in three-dimensional representations that qualitatively reproduce the essential features of the data as seen in Figs. 4(b) and 4(d) with  $\alpha = 0.5$  pointing to an Auger electron with  $s$  and  $d$  wave character. This analysis, however, does not reproduce the forward-backward anisotropy observed along the spectrometer axis

as shown in Fig. 5. This effect rather seems to be due to scattering of the photoelectron in the anisotropic field of the molecule on its way out.

In summary, we measured the 3D angular distributions of  $O^+$  ions produced by the autoionization of aligned excited atoms in the photodissociation of oriented oxygen molecules. Treatment of the resonance process in a two-step model concerning excitation and decay makes it possible to factorize the observed anisotropy of the fragment ion distribution in terms of the product of two angular distributions, that for a molecular alignment in the laboratory frame and that of electron waves in the molecular frame. The latter are described as superposition of atomic waves with different angular momentum produced in the autoionization process. Our results for the molecular alignment are interpreted in terms of a predominantly perpendicular  $^3\Sigma_g^- \rightarrow ^3\Pi_u$  transition followed by fast dissociation into an excited and ground-state oxygen atom. The coincident electron is essentially emitted into a  $\sigma_g$  wave with a  $s$  and  $d$  wave character. A small forward-backward asymmetry is observed and interpreted in terms of intramolecular scattering of the Auger electron from a specific atom due to the site-specific localization of the excited electron due to the dissociation process.

We acknowledge the support from different EC programs, and we thank the staff of LURE and LCAM workshops for their financial and technical support. We also thank J.C. Brenot and M. Vervloet for their help with this work. One of us (A.G.) acknowledges the financial support from LURE and the Deutsche Forschungsgemeinschaft.

- 
- [1] P.M. Dehmer and W. Chupka, J. Chem. Phys. **62**, 4525 (1975).
  - [2] A. A. Wills, A. A. Cafolla, and J. Comer, J. Phys. B **24**, 3989 (1991).
  - [3] M. Ukai *et al.*, Phys. Rev. Lett. **74**, 239 (1995).
  - [4] P.-M. Guyon *et al.*, Phys. Rev. Lett. **67**, 675 (1991).
  - [5] A. V. Golovin, Opt. Spectrosc. **71**, 537 (1991).
  - [6] A. V. Golovin, N. A. Cherepkov, and V. V. Kuznetsov, Z. Phys. D **24**, 371 (1992).
  - [7] E. Shigemasa *et al.*, Phys. Rev. Lett. **74**, 359 (1995).
  - [8] P.-M. Guyon *et al.*, Phys. Rev. Lett. **76**, 600 (1996).
  - [9] R. E. Huffman, J. C. Larrabee, and Y. Tanaka, J. Chem. Phys. **47**, 4462 (1967).
  - [10] U. Becker *et al.*, Phys. Rev. A **47**, R767 (1993).
  - [11] J. Dehmer and D. Dill, Phys. Rev. A **18**, 164 (1978).
  - [12] M. Richard-Viard, A. Delboulb e, and M. Vervloet, Chem. Phys. **209**, 159 (1996).
  - [13] N. Saito *et al.*, Phys. Rev. A **54**, 2004 (1996).
  - [14] W. C. Wiley and H. McLaren, Rev. Sci. Instrum. **26**, 1150 (1955).